AMERICAN ACADEMY OF OPHTHALMOLOGY®

Linking OCT, Angiographic, and Photographic Lesion Components in Neovascular Age-Related Macular Degeneration

*Cynthia A. Toth, MD,[1,4] Vincent Tai, MS,[1] Stephanie J. Chiu, PhD,[1] Katrina Winter, BS,[1] Monica B. Sevilla, MS,[1] Ebenezer Daniel, MBBS, PhD,[2] Juan E. Grunwald, MD,[2] Glenn J. Jaffe, MD,[1] Daniel F. Martin, MD,[3] Gui-shuang Ying, PhD,[2] Maxwell Pistilli, MS,[2] Sina Farsiu, PhD,[4] Maureen G. Maguire, PhD,[2] for the Comparison of Age-Related Macular Degeneration Treatments Trials (CATT) Research Group**

Purpose: To develop methods to make precise comparisons of specific retinal features between and within spectral-domain (SD) OCT images, color fundus photography (CFP) images, and fluorescein angiography (FA) images in eyes treated with anti–vascular endothelial growth factor (VEGF) agents for neovascular age-related macular degeneration (nAMD).

Design: Retrospective study.

Participants: Patients with good study-eye images at the 104-week visit in the Comparison of Age-Related Macular Degeneration Treatments Trials.

Methods: Graders reviewed CFP and FA images and delineated areas of fibrotic or nonfibrotic scar and geographic atrophy (GA) or non-GA. Other graders reviewed SD-OCT images and delineated retinal and subretinal lesion characteristics. Using newly developed custom software and graphic user interfaces, the presence and thickness of each feature at each pixel on the en face view was determined.

Main Outcome Measures: Spectral-domain OCT findings versus CFP and FA lesion components from regional overlays.

Results: Per-eye distribution and thickness of SD-OCT features within CFP- and FA-established areas of scar and atrophy can be determined precisely, can be displayed in multiple formats, and can be extracted into pixel-specific data sets. These methods enable statistical analysis of imaging results within eyes and across eyes of different patients. For example, photoreceptor loss, subretinal lesion material, and thicknesses of photoreceptor layer and subretinal material across those SD-OCT features can be related precisely to CFP and FA regions of scar or atrophy.

Conclusions: Methods to integrate qualitative and quantitative retinal and subretinal changes to coincide with photographic and angiographic designations of the nAMD lesion areas and sequelae are integral for accurate assessments of posttreatment retinal morphologic features. These may lead to better understanding of disease progression and improved treatment strategies. *Ophthalmology Retina 2018;2:481-493 © 2017 by the American Academy of Ophthalmology*

Supplemental material available at www.ophthalmologyretina.org.

Eyes with neovascular age-related macular degeneration (nAMD) treated with anti–vascular endothelial growth factor (anti-VEGF) agents demonstrate many interrelated retinal architecture changes. A single eye may have changes related to active neovascularization, atrophy, and scarring. These processes may be monitored by several imaging methods, most often stereoscopic color photography, stereoscopic fluorescein angiography (FA), and OCT. Combining the information from these different methods with high accuracy and precision allows for developing, proving, and disproving hypotheses regarding the development and progression of neovascularization, atrophy, and scarring.

In the Comparison of Age-Related Macular Degeneration Treatments Trials (CATT) and other longitudinal studies of the outcomes of anti-VEGF treatment for nAMD, both geographic atrophy (GA) and scar have been reported to develop frequently[1–3] and to be associated with poor visual acuity.[4,5] The changes accompanying these processes are poorly understood. Mowatt et al[6] pointed to the need for integrated information on the performance of spectral-domain (SD) OCT compared with FA for diagnosis and monitoring of active and inactive nAMD. Schmidt-Erfurth and Waldstein[7] pointed to the need for integrated analysis of all structural and functional features to determine retinal

https://doi.org/10.1016/j.oret.2017.09.016
ISSN 2468-6530/17

biomarkers that could guide efficient individualized treatment of nAMD. Castillo et al,[8] in a review, recognized the disagreement between OCT and FA in detecting active disease and the paucity of studies directly comparing the tests in the same population. To date, identification of the relative size and regional distribution across the macula of multiple lesion components visible on OCT compared with the relative size and regional distribution of lesion components visible on color fundus photography (CFP) and FA has been performed manually and for only 1 or a few selected lesion components.

To extract this important information from OCT, CFP, and FA imaging in CATT, we developed novel methods and software to register and analyze the regional distribution of SD-OCT retinal and subretinal data and of CFP and FA data. With these methods of registration, pixel-by-pixel analysis, and overview analysis, researchers will be able to integrate the different imaging methods to understand better the range of neovascular lesion components. This will be useful in future studies of the pathophysiologic features of nAMD, because local precursors can be mapped to the regional progression and outcomes of nAMD. Thus, data from future studies using these methods will be useful to clinicians who need to predict and monitor response to nAMD treatment and to those developing novel therapies for nAMD.

Methods

The CATT participants and methods have been described in previous publications.[9,10] CATT was registered with ClinicalTrials.gov (identifier, NCT00593450). Enrollment extended across 43 clinical centers in the United States from February 2008 through December 2009. The study was approved by an institutional review board associated with each center and complied with the Health Insurance Portability and Accountability Act regulations. The study was performed in accordance with the tenents of the Declaration of Helsinki. All participants provided written informed consent. The image analysis methods were developed using a subset of images from CATT.

At baseline in CATT, participants underwent bilateral stereo CFP, FA, and time-domain OCT. Color fundus photography and FA along with OCT were performed again at 1, 2, and 5 years. Spectral-domain OCT imaging was conducted in many of the CATT participants after the year 1 visit.[11] In CATT, year 2 (104-week visit) scans were captured either with time-domain OCT methods or SD-OCT using Cirrus (Carl Zeiss Meditech, Dublin, CA) or Spectralis (Heidelberg Engineering, Heidelberg, Germany) systems. Only Cirrus and Spectralis SD-OCT scans were used in this overlay study. Images were acquired on the Cirrus device with the scan pattern of 6 × 6-mm macular volume cube with 128 horizontal line scans. Images were acquired on Spectralis OCT devices with 3 scan patterns: 20° × 20° macular volume cube with 49 horizontal line scans, 30° × 30° macular volume cube with 49 horizontal line scans, and 30° × 30° macular volume cube with 97 horizontal line scans. All scan patterns have 512 A-scans per line scan.

Photographic images were evaluated by the CATT Fundus Photography Reading Center at the University of Pennsylvania, and OCT images were evaluated by the CATT OCT Reading Center at the Duke Advanced Research in SS/SD-OCT Imaging Laboratory. Graders at each reading center were masked to the assessment from the other reading center. Four main features identifiable on stereo CFP and FA images of eyes treated with anti-VEGF agents were identified for in-depth evaluation (Table 1; see "Photographic Analysis," below): GA, non-GA, fibrotic scar, and nonfibrotic scar. Images of eyes at the 104-week CATT visit with these features present on CFP and with OCT images of sufficient quality to grade were selected for development and illustration of the methods described in this article.

Photographic Analysis

Two graders at the CATT Fundus Photography Reading Center each viewed CFP and FA images at that visit. For each of the features listed in Table 1, the graders outlined the area of the features on a frame from the FA image; this drawing was considered a layer. The same frame from the FA image was used for all layers. The FA frame was selected based on the clarity of the image, the presence of at least three quarters of the optic disc in the image, and having the most features of interest among those present on the entire angiogram. The FA image was imported into Photoshop (Photoshop CS3; Adobe Systems, San Jose, CA), and each of the CFP or FA components was outlined. Delineations on the FA image were performed on one monitor, whereas color, red-free, and fluorescein images of the same visit were viewed on an adjacent monitor. Information from all images was ascertained to mark the foveal center and center of the optic disc and to outline each type of morphologic characteristic. Qualitative and quantitative grading of fundus morphologic and FA characteristics in CATT have been shown to have good reproducibility.[12]

The foveal center was determined by identifying an area of increased pigmentation in the middle of the macular region on the color image and the geometric center of the area surrounded by the termination of the smallest visible perifoveal vessels seen clearly in the early FA transit phase or red-free image. In poor-quality images, baseline images having fluid and hemorrhage, and in follow-up images that had scar or atrophy at the mid-macular region, the best approximation of the foveal center was made and marked. A 6-mm diameter circular template centered on the foveal center was applied, and morphologic features of the total choroidal neovascularization lesion were delineated in 13 (11 components plus the fovea and disc center) labeled layers within that ring. The total choroidal neovascularization lesion components included choroidal neovascularization, hemorrhage, fibrotic scar, nonfibrotic scar, serous pigment epithelial detachment, blocked fluorescence, GA, non-GA, retinal angiomatous proliferation, and retinal pigment epithelium (RPE) tear (Table 1). Each of these 11 components was exclusive at any single location, so that a site could not be assigned 2 components.

The outline of each layer, representing 1 morphologic feature, was a unique color available in the Photoshop software. Outlining a particular morphologic feature was achieved using a single unbroken line. If the same morphologic feature was observed in several areas (e.g., multiple GA lesions), each area was drawn. Any of the defined morphologic features completely or partially within the circular template or touching the circle were drawn, even if they extended beyond the template.

OCT Analysis

Trained readers at the Duke Advanced Research in SS/SD-OCT Imaging Laboratory used proprietary software, the Duke OCT Retinal Analysis Program Marking Code version 61.4.2 (MATLAB R2012a; Mathworks, Natick, MA), to mark the foveal center based on the deepest site in the foveal pit for each scan, the photoreceptor bulge, or the best estimate. Readers also marked the lateral extent of all morphologic features observed across the full extent of each B-scan (Fig 1) using defined criteria listed in

Table 1. Definitions of Color Fundus Photographic and Fluorescein Angiographic Lesion Component Morphologic Features

Color Fundus Photographic and Fluorescein Angiographic Components	Definition
Fibrotic scar	Sheets or mounds of white or yellowish material on color photographs; some fibrotic scars or portions of the scar may stain and show hyperfluorescence, whereas others may obstruct the view of the underlying choroidal flush and therefore be hypofluorescent; based mainly on features observed on color images.
Nonfibrotic scar	An area of flat hypopigmentation partially or completely surrounded by an area of hyperpigmentation on color images with corresponding hyperfluorescence and hypofluorescence on FA; in some instances, the central hypopigmentation is absent. The hyperpigmentation often corresponds to the outer extent of a classic CNV.
Geographic atrophy	Sharply defined areas of partial or complete depigmentation of the RPE larger than 250 μm, typically exposing the choroidal blood vessels; late FA shows well-circumscribed areas of hyperfluorescence corresponding to the hypopigmented areas of the color image.
Non–geographic atrophy	Hypopigmentation and hyperpigmentation on color images that typically corresponds to hyperfluorescence and hypofluorescence, respectively, on FA; borders not sharply defined and choroidal vessels not visible. When areas of hyperfluorescence do not correspond exactly to pigmentary changes on color images, they are included as NGA.
Blocked fluorescence	Areas of hypofluorescence on FA not corresponding to hemorrhage or pigmentation on color or red-free images (a risk factor for fibrotic scar formation and associated with a lower risk of geographic atrophy).[1,2]
CNV (classic, occult, or mixed)	Classic CNV is characterized by well-demarcated early-phase fluorescein leakage that progressively becomes larger and in the late phase obscures the borders of the CNV. In some cases, a lacy network of neovascularization is seen before leakage appears. When combined with fibrosis, classic CNV may leak in the mid phase, and the leakage may not be intensive. Classic is outlined on FA just before leakage begins. Occult CNV is characterized by ill-defined areas of fluorescein leakage that begin toward the end of the mid phase. In some cases, there is leakage only in the late phase accompanied by intense stippling. Occult CNV typically is outlined on a late-phase image to include areas of persistent late staining and leakage. Mixed lesions are drawn on a frame of FA that includes a combination of these characteristics.
Hemorrhage	Hemorrhage is seen as bright red superficial blood or as deeper, darker circumscribed blood obscuring the choroidal flush and appearing as corresponding hypofluorescent patches in FA. Extent is based on color and red-free images, and the area where they are present is drawn; all areas of hemorrhage, regardless of association with CNV or RAP or the level (retinal, subretinal, or sub-RPE), are included.
Retinal angiomatous proliferation	Determined by the presence of intraretinal fluorescein leakage (hot spot) in the early transit images of the FA. The RAP lesion also includes other characteristics such as superficial retinal hemorrhages, PED (SPED, FV-PED), lipid, and anastomosis of retinal vessels with other retinal vessels or with the CNV lesion. The hot spot is the primary constituent of the RAP lesion, and the other features may or may not be present.
Retinal pigment epithelium tear	Hypofluorescence on FA where the flap of the tear is located and hyperfluorescence where RPE has retracted, exposing the underlying choroid. Both the flap and the pigment denuded area are included. If fibrosis has formed within the area of the tear, it is included in the scar layer outline.
Serous pigment epithelial detachment	An area of increasing hyperfluorescence typically as a rounded lesion that is homogenously smooth and well circumscribed.
Total CNV lesion	Includes CNV, hemorrhage, scar (fibrotic or nonfibrotic), SPED, FV-SPED, blocked fluorescence, NGA, RAP, GA, and RPE tear.

CNV = choroidal neovascularization; FA = fluorescein angiography; FV-PED = fibrovascular pigment epithelial detachment; FV-SPED = fibrovascular serous pigment epithelial detachment; GA = geographic atrophy; NGA = non–geographic atrophy; PED = pigment epithelial detachment; RAP = retinal angiomatous proliferation; RPE = retinal pigment epithelium; SPED = serous pigment epithelial detachment.

Table 2. Although most SD-OCT features could be colocalized at the same en face location (e.g., intraretinal fluid could be present at the same en face location as subretinal highly reflective material [SHRM]) by definition, several components (e.g., complete RPE and outer retinal atrophy[13] and SHRM) were mutually exclusive, as listed in the third column of Table 2. Qualitative and quantitative grading of fundus morphologic characteristics on OCT in CATT have been shown to have good reproducibility.[11,14]

Cirrus and Spectralis volumes were segmented automatically using Duke OCT Retinal Analysis Program Marking Code version 61.9, which delineated the inner aspect of the internal limiting membrane, the inner aspect of the outer plexiform layer (OPL), the inner aspect of the subretinal complex defined below, and the outer aspect of Bruch's membrane. Because OCT volumes varied in scan dimension (from 5.4 to 6 mm) and the fovea was not consistently at the precise center of the scan, a 6-mm diameter circular region of interest (ROI) would result in areas lacking OCT data. Thus, a 5-mm diameter circular ROI centered on the foveal center of the segmented volume scans was used as the ROI for final overlay analysis. Trained readers reviewed the automated segmentation and corrected errors within this final 5-mm diameter ROI.

Across the final ROI, the neurosensory retinal thickness was measured from the inner aspect of the internal limiting membrane to the inner aspect of the subretinal complex (Fig 2, between lines 1 and 3). Thickness of inner retinal layers included the internal limiting membrane to the inner border of the OPL (Fig 2, between lines 1 and 2). Thickness of the photoreceptor layer included the OPL to the inner border of the subretinal complex (Fig 2, between lines 2 and 3). Based on previous published definitions and with the inclusion of nAMD lesion components,

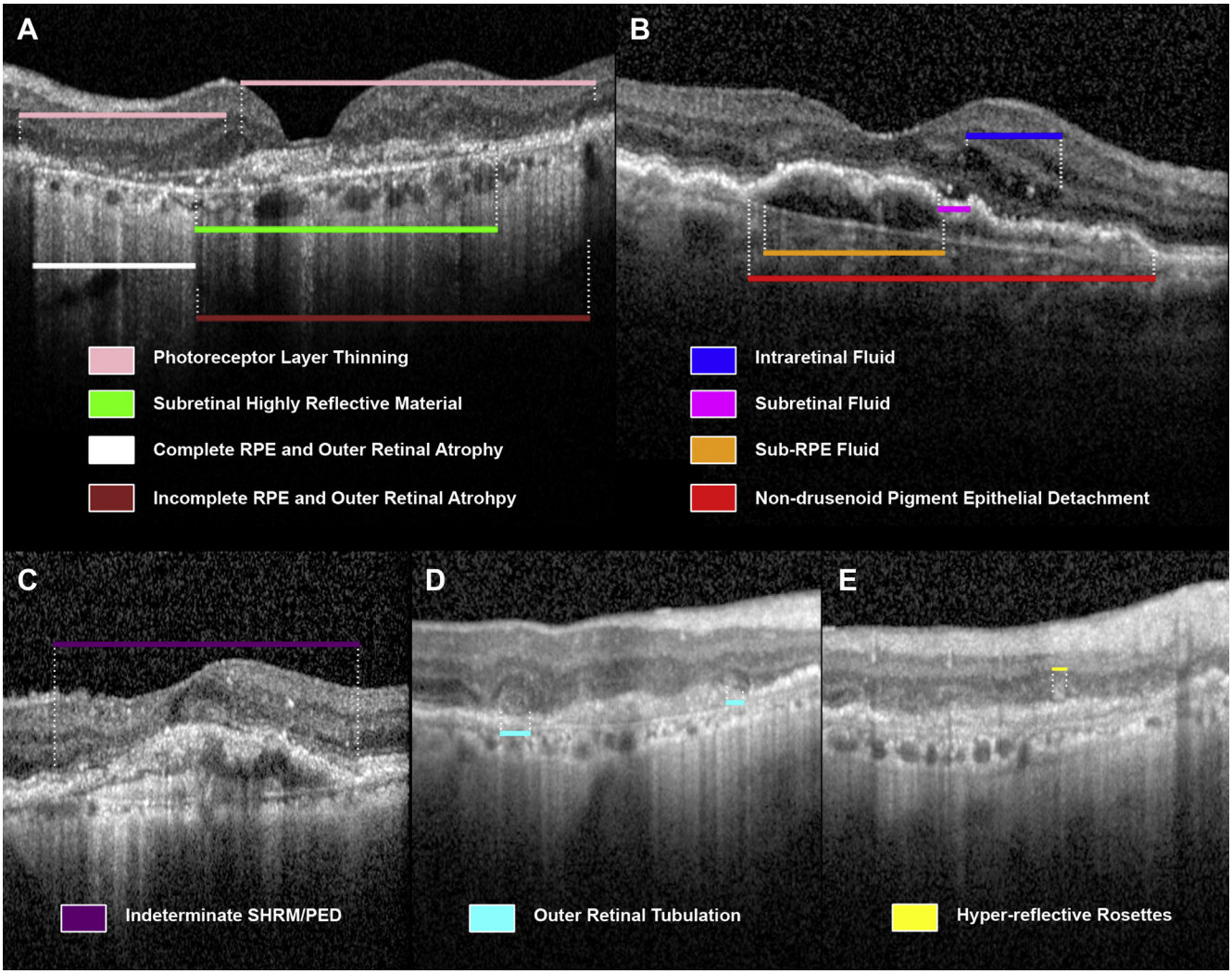

Figure 1. Spectral-domain OCT scans showing: (**A**) photoreceptor layer thinning (*pink*), subretinal highly reflective material (SHRM; *green*), complete retinal pigment epithelium (RPE) and outer retinal atrophy (*white*), and incomplete RPE and outer retinal atrophy (*brown*); (**B**) intraretinal fluid (*blue*), subretinal fluid (*magenta*), sub-RPE fluid (*orange*), and nondrusenoid pigment epithelial detachment (PED; *red*); (**C**) hyperreflective rosettes (*yellow*); (**D**) outer retinal tabulation (*cyan*); and (**E**) indeterminate SHRM or PED (*purple*).

the subretinal complex was termed the *retinal pigment epithelium plus drusen plus lesion complex* (RPEDLC) and included the RPE, all drusen material, whether above (subretinal drusenoid deposits) or below the RPE (basal linear, basal laminar deposits, and drusen), in addition to any subretinal lesion and subretinal fluid and sub-RPE lesion plus sub-RPE fluid. The RPEDLC thickness extended from the inner border of the complex to the outer aspect of Bruch's membrane (Fig 2, between lines 3 and 4). The semiautomated segmentation of retinal layers has been shown to have good reproducibility in eyes with AMD[15–17]; reproducibility for presence and location of SHRM has been shown to be excellent, and thickness agreement at multiple points over SHRM was shown to range from 4 to 15 μm.[18]

Photographic and OCT Overlay Image Registration

The original study design planned for alignment of the foveal center for registration between the SD-OCT images and the FA frame and then size correction of the FA frame (and image layers) based on assigning a standard distance (4.5 mm) as the distance from the foveal center to the center of the optic nerve. This first approach was found to be insufficiently accurate for size matching the FA image to the OCT image; therefore, after aligning the foveal center, we corrected the magnification of the FA frame by manually registering (without warping or skew) the vascular pattern over the vessels of the retinal view from the SD-OCT image.

Custom MATLAB software (CATTREG version 2.9) with a graphic user interface was designed to register and compare OCT markings side by side with CFP or FA markings and to extract en face overlays of the SD-OCT, CFP, and FA data pixel by pixel. Graders registered OCT volumes to their corresponding FA images, and the software then registered and overlaid the associated markings. The SD-OCT volumes varied in scan density and pixel resolution, with 49 or 97 B-scans in each Spectralis volume and 128 B-scans in each Cirrus macular cube. Both OCT and FA data were standardized to 1001 × 1001-pixel matrix maps centered at the fovea to facilitate comparison. For each patient, the program

Table 2. Definitions of OCT Regional Component Morphologic Features

OCT Regional Morphologic Feature	Definition	Mutually Exclusive at the Same Pixel Location
Intraretinal fluid	Low reflective round or oval cystic spaces within the neurosensory retina and without the characteristics of ORT.	
Outer retinal tubulation	Round or tubular low-reflective structures with a hyperreflective lumen around the outside. There may be bright foci within the structure.	Hyperreflective rosettes
Hyperreflective rosettes	Large hyperreflective foci grouping in the presence of GA or CNV	ORT
Subretinal fluid	Low reflective area at the level below the neurosensory retina but above the RPE. It may have a turbid appearance in part, but remains less reflective than SHRM.	
Subretinal highly reflective material	Mixed moderately to highly reflective material at or above the RPE layer and extending upward toward the retina, but not within the neurosensory retina. This pathologic feature can be dense and highly reflective or poorly defined, but is not defined as a known retinal structure.	cRORA
Nondrusenoid pigment epithelial detachment	Pigment epithelial elevation of more than 1000 μm horizontally along Bruch's membrane and not identified as strictly drusenoid material within or multiple drusen that have coalesced to form a large drusenoid complex.	cRORA
Indeterminate SHRM or PED	Subretinal lesion that cannot be distinguished clearly as either SHRM or PED because of scan quality or because the pathologic features are not clearly defined.	cRORA
Sub-RPE fluid	Low reflectivity located beneath the RPE but within an area of RPE elevation and would include serous PED; a low-reflective drusen is not considered sub-RPE fluid.	cRORA
Incomplete RPE and outer retinal atrophy (iRORA)	Increased OCT signal extending into the choroid with a higher intensity than surrounding penetrating signal, but with persisting RPE, outer retinal layers, or lesion or debris above. OPL dipping (photoreceptor layer thinning) is common in these areas, but should not extend all the way to Bruch's membrane.	cRORA
Complete RPE and outer retinal atrophy	RPE absence with increased signal extending into the choroid with a higher intensity than surrounding choroidal signal with absent photoreceptor layer. OPL dipping is always visible in these areas.	SHRM, PED, PED or SHRM, sub-RPE fluid, iRORA
Photoreceptor layer thinning	The inner boundary of the outer plexiform layer dips toward Bruch's membrane and RPE and below what is expected for the normal contour at that location. This is seen typically over areas of pathologic features such as drusen, SHRM, PED, cRORA, and iRORA.	

CNV = choroidal neovascularization; cRORA = complete retinal pigment epithelium and outer retinal atrophy; GA = geographic atrophy; iRORA = incomplete retinal pigment epithelium and outer retinal atrophy; OPL = outer plexiform layer; ORT = outer retinal tubulation; PED = pigment epithelial detachment; RPE = retinal pigment epithelium; SHRM = subretinal highly reflective material.

generated a registered OCT retinal view and angiographic frame that were fovea centered, 1001 × 1001 pixels and 6 μm/pixel in resolution. Interpolation was performed between OCT B-scans because the distance between each B-scan was more than 1 pixel (6 μm). After image registration and standardization, the program output a data table containing each pixel's location on the standardized grid and a binary value specifying whether the OCT, CFP, or FA component was present or absent for that pixel. For this

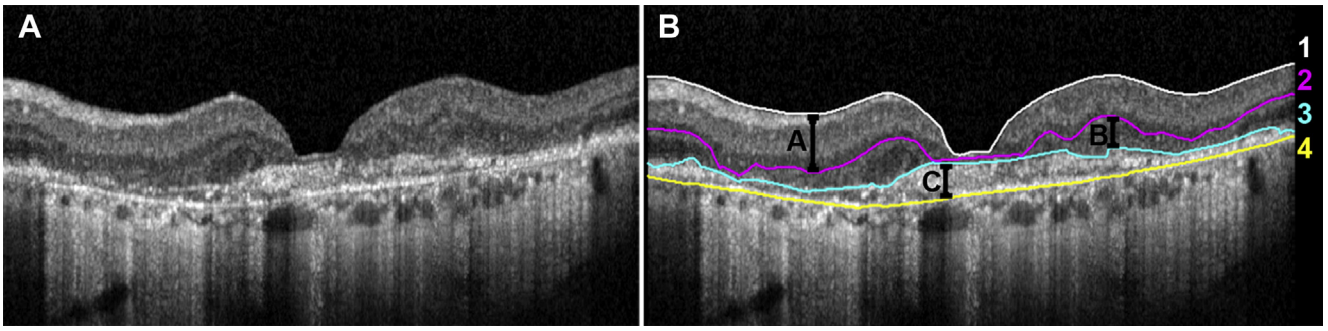

Figure 2. Segmentation of the retina using the Duke Optical Coherence Tomography Retinal Analysis Program version 61.9 across the foveal center demonstrating (**A**) delineation of the inner border of the internal limiting membrane, inner border of the outer plexiform layer, inner border of the retinal pigment epithelium plus drusen plus lesion complex (RPEDLC), and outer border of Bruch's membrane, which results in (**B**) inner retinal layer (**A**), photoreceptor layer (**B**), neurosensory retinal layer (**A**+**B**), and RPEDLC (**C**).

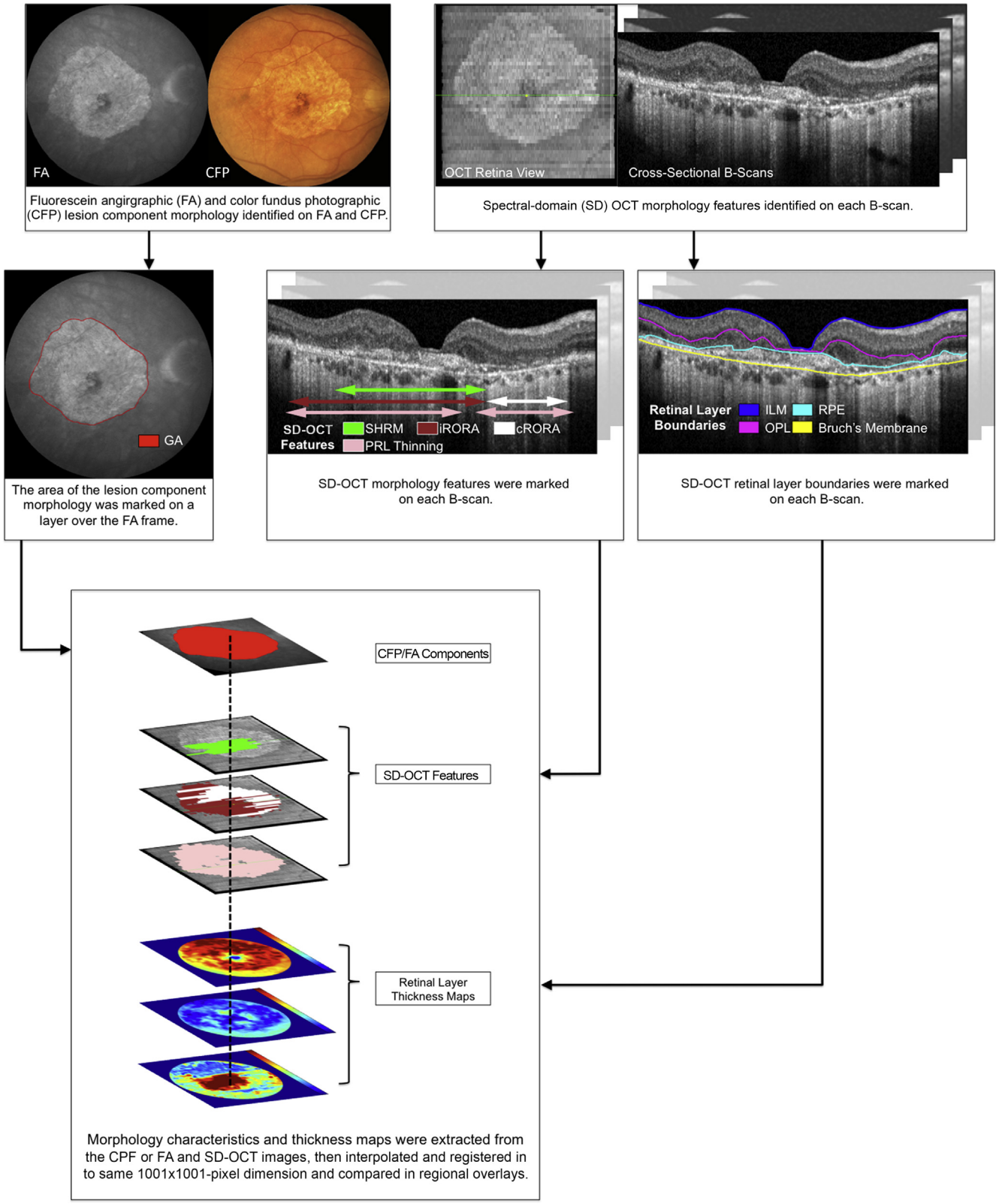

Figure 3. Workflow diagram showing image analysis and image process method. CFP = color fundus photography; cRORA = complete retinal pigment epithelium and outer retinal atrophy; FA = fluorescein angiography; GA = geographic atrophy; ILM = internal limiting membrane; iRORA = incomplete retinal pigment epithelium and outer retinal atrophy; OPL = outer plexiform layer; PRL = photoreceptor layer; RPE = retinal pigment epithelium; SHRM = subretinal highly reflective material.

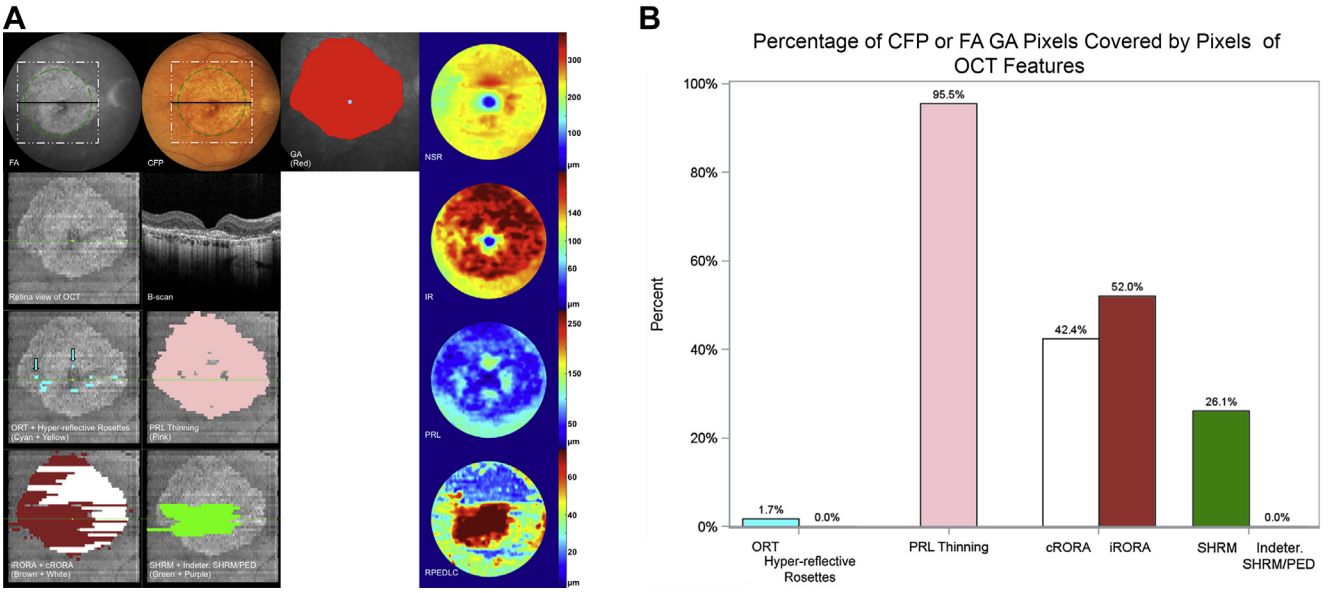

Figure 4. **A**, Images from a representative macula in an eye with geographic atrophy (GA) and a history of neovascular age-related macular degeneration obtained 2 years after the start of anti–vascular endothelial growth factor therapy. Geographic atrophy was identified on color fundus photograph (CFP; row 1, column 2) and fluorescein angiography (FA; row 1, column 1, representative frame) review. The area of GA was marked on a layer over the FA frame (row 1, column 3). The FA image was sized and registered to the spectral-domain (SD) OCT retinal image (row 2, column 1). A representative B-scan (row 2, column 2) demonstrates the SD-OCT morphologic features at the foveal center. Spectral-domain OCT morphologic components were marked manually on each B-scan to delineate areas of OCT morphologic features (rows 3 and 4, columns 1 and 2), which included outer retinal tubularization (ORT; row 3, column 1), photoreceptor layer (PRL) thinning (row 3, column 2), incomplete retinal pigment epithelium (RPE) and outer retinal atrophy (iRORA; *white*, row 4, column 1) and complete RPE and outer retinal atrophy (cRORA; *red-brown*, row 4, column 1), and subretinal highly reflective material (SHRM; row 4, column 2). Color maps represent retinal and subretinal layer thicknesses (column 4). Photoreceptor layer thinning (*dark blue*, row 3 column 4) corresponded to CFP or FA GA, iRORA plus cRORA, better than total neurosensory retina (NSR) thinning (row 1, column 4), and retinal pigment epithelium plus drusen plus lesion complex (RPEDLC) thinning (*dark blue*, row 4, column 4). The SHRM and pigment epithelial detachment (PED) resulted in an area of thickened RPEDLC (*dark red*, row 4, column 4). **B**, Graph showing percentage of CFP- or FA-determined GA lesion pixels covered by pixels of OCT features. IR = inner retina.

analysis, all eyes were oriented as a right eye to allow for inter-method, intervisit, and interpatient comparisons.

We calculated the mean layer thickness for the RPEDLC, retina, and inner and outer retina within the 5-mm diameter ROI. To calculate these, we centered the layer boundary maps at the fovea and generated thickness maps of 1001 × 1001 pixels to achieve equivalent resolutions in both en face (*x*-*y*) directions. Thickness values were converted from pixels to micrometers according to the appropriate OCT imaging axial resolutions. In addition to lesion components, we designated nonlesion regions as CFP, FA, or OCT areas without marked lesion components. We calculated the mean thickness of the RPEDLC for each of the 4 designated CFP or FA components: GA, fibrotic scar, non-GA, and nonfibrotic scar; we also calculated the percentage of the CFP or FA component area that was occupied by different OCT features.

Results

Analysis of Spectral-Domain OCT Features and Color Fundus Photography Components of Neovascular Age-Related Macular Degeneration

This study developed and systematically applied novel methods for pixel correspondence across images that enabled location-specific analysis within corresponding SD-OCT, CFP, or FA images. The workflow of image processing is depicted in Figure 3 and is illustrated in the 4 examples in Figures 4 to 7. In those figures, we provide representative macular overlays to demonstrate the steps of the process and usefulness of this visualization method in each of the 4 CFP or FA component areas: GA, fibrotic scar, non-GA, and nonfibrotic scar. The potential usefulness of this method for visualizing and evaluating the multilayer effects of nAMD 2 years after the start of anti-VEGF therapy is demonstrated in Figures 4A, 5A, 6A, and 7A. In addition to the complex visualization, the corresponding pixel-to-pixel report for each macula provides a summary of the data for each eye that can be extracted for overview (Figs 4B, 5B, 6B, and 7B) and for statistical analyses across multiple eyes.

In imaging from the 104-week CATT visit (represented by the FA frame and color photograph in Figs 4A, 5A, 6A, and 7A), the component area was marked on a representative FA frame that was magnified (row 1, column 3) to match in size and to register to the area of the OCT retinal view (row 2, column 1). A representative foveal B-scan from the OCT scan, located at the green line on the OCT retinal view, is shown in each composite figure. The OCT features each were projected from the OCT grader markings onto the OCT retinal view (multiple frames in Figs 4A, 5A, 6A, and 7A), and these often appear as parallel hatched lines because they represent markings from individual B-scans. Because all eyes do not have all features present, there are some blank squares in the representative figures.

The data processing resulted in comparably sized and registered CFP, FA, or OCT data in 1001 × 1001-pixel areas, across which we could calculate the percentage of the CFP or FA lesion component covered by OCT features. Analysis of similarly labeled

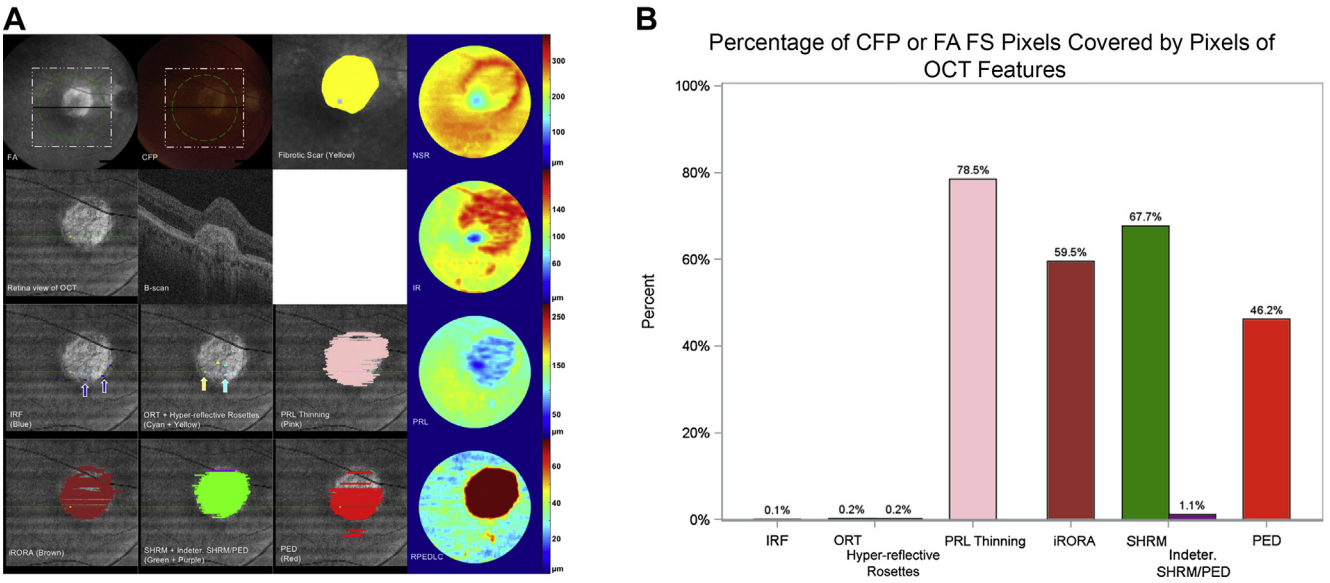

Figure 5. **A**, Images from a representative macula in an eye with a history of neovascular age-related macular degeneration obtained 2 years after the start of anti–vascular endothelial growth factor therapy. Fibrotic scar was identified on color fundus photography (CFP; row 1, column 2) and fluorescein angiography (FA; row 1, column 1, representative frame) review; the area of scar was marked on a layer over the FA frame (row 1, column 3). The FA image was registered to the spectral-domain (SD) OCT retinal image (row 2, column 1). A representative B-scan (row 2, column 2) demonstrates 1 line of the SD-OCT morphologic features that were marked manually on each B-scan. Retinal changes on SD-OCT included intraretinal fluid (IRF; row 3, column 1), outer retinal tubularization (ORT; row 3, column 2), and photoreceptor layer (PRL) thinning (row 3, column 3). The latter corresponded to photoreceptor thinning on segmented scans (*dark blue*, row 3, column 4). Incomplete retinal pigment epithelium (RPE) and outer retinal atrophy (iRORA; *brown*, row 4, column 1) was present despite the overlying thick subretinal highly reflective material (SHRM), indeterminate SHRM or pigment epithelial detachment (PED; row 4, column 2), and PED (row 4, column 3). The thickness of the SHRM and PED complex is reflected in the color map as an area of thickened RPE plus drusen plus lesion complex (RPEDLC; *dark red*, row 4, column 4). **B**, Graph showing the percentage of CFP- or FA-determined fibrotic scar (FS) lesion pixels covered by pixels of OCT features. IR = inner retina; NSR = neurosensory retina.

CFP, FA, or OCT pixels, including pixels containing thickness measurements from semiautomated OCT segmentation (column 4 of composite figures: retina, inner retina, photoreceptor layer, and RPEDLC in rows 1–4, respectively), thus could proceed across multiple eyes. The positions of the pixels were known relative to the foveal center and nasal, temporal, superior, and inferior locations, so analyses also could include relative location.

OCT Features in an Area of Color Fundus Photography- or Fluorescein Angiography-Designated Geographic Atrophy

Within areas that appeared as GA on CFP or FA at the 104-week CATT visit, we often found subretinal OCT features that were atypical for GA. In the example in Figure 4A, extended across the center of the GA area on the CFP or FA image we found SHRM on the OCT (Fig 4A, B-scan) that was mapped as a green area on the retinal view and that also corresponded to the area of thickened RPEDLC (dark red in the RPEDLC thickness map). The thickness of the RPEDLC for the area of all pixels designated as SHRM versus non-SHRM within the GA could be reported, as could the thickness for all pixels designated as GA. For example, the mean RPEDLC for the pixels designated as GA was 42.4 μm (standard deviation, 25.3 μm), which subdivided into mean thickness for those GA pixels with SHRM of 73.8 μm (standard deviation, 21.4 μm) versus non-SHRM of 33.5 μm (standard deviation, 13.8 μm). Such analyses can be performed for similarly labeled pixels across multiple eyes.

In almost all of the area of CFP- or FA-designated GA, including across pixels with SHRM, there was increased choroidal signal on OCT. Pixels with increase in choroidal signal, but with persisting reflective material in the RPE location (or even SHRM), were designated as incomplete RPE and outer retinal atrophy (iRORA; Fig 4A, red-brown area). In this eye, for example, iRORA extends beyond the SHRM because there are additional areas of increase in choroidal signal with persisting overlying material that seem to be comparable with RPE or RPE debris, but not consistent with SHRM. In the OCT retinal image (Fig 4A), regions of persisting RPE-type material showed more reflectance than the adjacent nonlesion areas, but less reflectance than the remaining areas of the CFP- or FA-designated GA.

In the remaining areas within the CFP- or FA-designated GA, there was an increase in choroidal signal along with RPE loss and photoreceptor thinning (Fig 4A, called *complete RPE and outer retinal atrophy*, white area). The RPEDLC layer was thinner in these areas (dark blue). Photoreceptor thinning, both qualitative (row 3, column 2, pink) and quantitative (row 3, column 4, darker blue areas), extended across areas with and without persisting RPE-type material. In contrast to the photoreceptor layer thinning, inner retinal layers were thickened (red) over the area of GA (Fig 4A, row 2, column 4). We also could determine the location of outer retinal tubulation (Fig 4A, teal) relative to SHRM and other features.

An example of the percent of the GA area covered by each SD-OCT feature is summarized in the graph in Fig 4B, for example, with approximately 95% of the GA pixels covered by OPL dipping with photoreceptor thinning and an increase in choroidal signal, although more than half of this was in areas with either

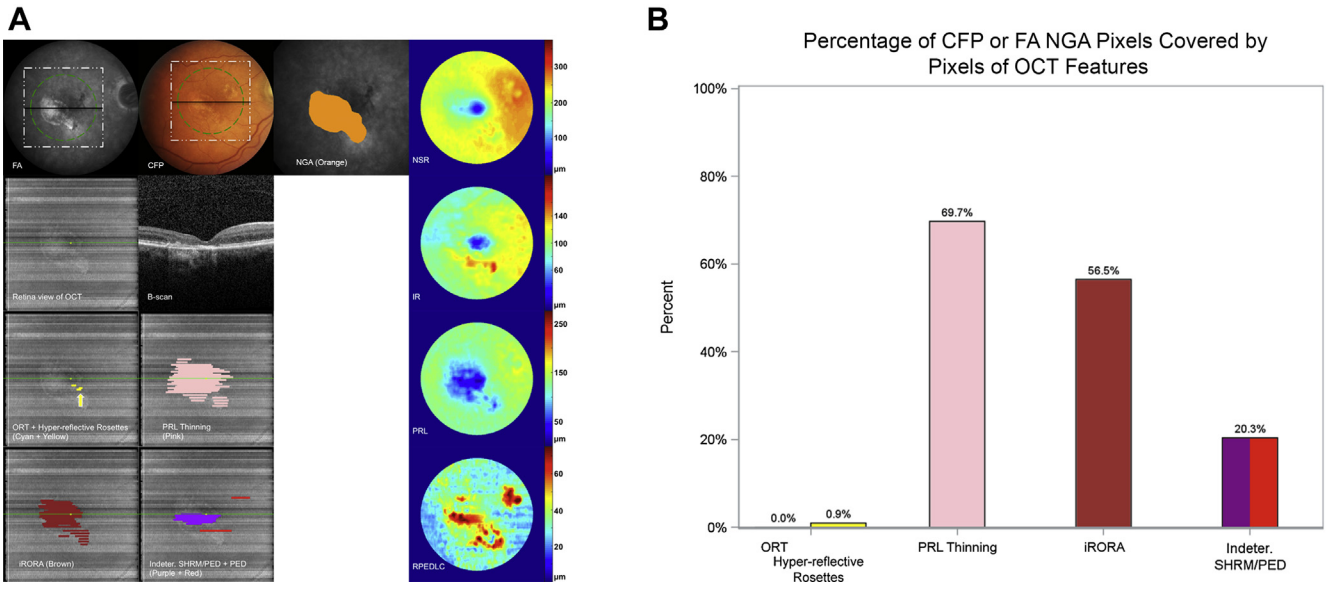

Figure 6. **A**, Images from a representative macula in an eye with a history of neovascular age-related macular degeneration obtained 2 years after the start of anti–vascular endothelial growth factor therapy. Non–geographic atrophy (NGA) was identified on color fundus photography (CFP; row 1, column 2) and fluorescein angiography (FA; row 1, column 1, representative frame) review; the area of NGA was marked on a layer over the FA frame (row 1, column 3). The FA image was registered to the spectral-domain (SD) OCT retinal image (row 2, column 1). A representative B-scan (row 2, column 2) demonstrates the SD-OCT morphologic features that were marked manually on each B-scan. The OCT morphologic features included hyperreflective rosettes (row 3, column 1), photoreceptor layer (PRL) thinning (row 3, column 2), incomplete retinal pigment epithelium (RPE) and outer retinal atrophy (iRORA; *brown*, row 4, column 1), and indeterminate subretinal highly reflective material (SHRM) or pigment epithelial detachment (PED) and PED (row 4, column 2). Color maps represent retinal and subretinal layer thicknesses (rows 2 and 4, column 4). Photoreceptor layer thinning (*dark blue*, row 3, column 4) corresponded to CFP or FA NGA and iRORA, better than neurosensory retinal thinning (row 2, column 4) and RPE plus drusen plus lesion complex (RPEDLC) thinning (*dark blue*, row 4, column 4). The indeterminate SHRM or PED and PED resulted in an area of thickened RPEDLC (*dark red*, row 4, column 4). **B**, Graph showing the percentage of CFP- or FA-determined NGA lesion pixels covered by pixels of OCT features. IR = inner retina; NSR = neurosensory retina; ORT = outer retinal tubularization.

RPE-type debris or lesion complex above the choroid (iRORA). A quarter of the area was covered by the SHRM.

OCT Features in an Area of Fibrotic Scar

The most prominent OCT features within this CFP or FA fibrotic scar area (Fig 5A, yellow) include photoreceptor thinning over a domed SHRM over a more subtle PED with underlying increase in choroidal signal (on OCT B-scan; Fig 5A). These map to respective areas on OCT maps in Figure 5A: photoreceptor thinning (pink), SHRM (green), PED (red), and iRORA (red-brown). We can align these with the pixels of corresponding thickness maps of the inner and outer retina and RPEDLC (Fig 5A, column 4) and extract, for example, that RPEDLC thickness is 151.2 μm (87.7 μm) across pixels designated on CFP or FA as fibrotic scar. Less common features such as intraretinal fluid (Fig 5A, navy) and outer retinal tubulation and hyperreflective rosettes (teal and yellow) also can be mapped.

The percent of the fibrotic scar area covered by each SD-OCT feature is summarized in the graph in Figure 5B. More than 78% of the fibrotic scar area has photoreceptor thinning and 59.5% of the scar has an increase in choroidal signal despite the overlying lesion. More than 65% of the scar area was covered by SHRM either alone or with PED.

OCT Features in an Area of Non–Geographic Atrophy

There were numerous subretinal OCT features within the CFP or FA non-GA area. Indeterminate SHRM or PED were visible on OCT B-scan (Fig 6A) and were mapped in the OCT demarcation (Fig 6A, purple and red). These corresponded to some of the areas of thickened RPEDLC (Fig 6A, dark red). Increased choroidal signal without loss of reflective material in the RPE location (Fig 6A, red-brown) involved most of the area.

In addition to the subretinal, RPE, and choroidal changes, SD-OCT also revealed patterns of retinal degeneration within the CFP- or FA-designated non-GA area. Outer retinal tubulation and hyperreflective rosettes (Fig 6A, teal and yellow) were present centrally. Photoreceptor layer thinning extended beyond the non-GA area on both qualitative (Fig 6A, pink) and quantitative (Fig 6A, dark blue) maps. Inner retinal layers were thickened over part of the area of photoreceptor thinning (Fig 6A), and total retinal thickness was decreased over a portion of the area (Fig 6A).

The percent of the non-GA area covered by each SD-OCT feature is summarized in the graph in Figure 6B. More than 69% of the non-GA area showed photoreceptor thinning and 58.5% of the non-GA area showed an increase in choroidal signal with overlying lesion. In the non-GA area, 20.3% was covered by indeterminate SHRM or PED or with PED. The RPEDLC thickness inside the 5-mm diameter ROI, meaning within the CFP or FA area designated as non-GA, was 46.6 μm (standard deviation, 11.1 μm).

OCT Features in an Area of Nonfibrotic Scar

There were numerous subretinal OCT features within the CFP or FA nonfibrotic scar area. Domed fibrotic PED also had focal overlying SHRM and minimal subretinal fluid on OCT B-scan (Fig 7A, SHRM, PED, and SRF). These corresponded to the area

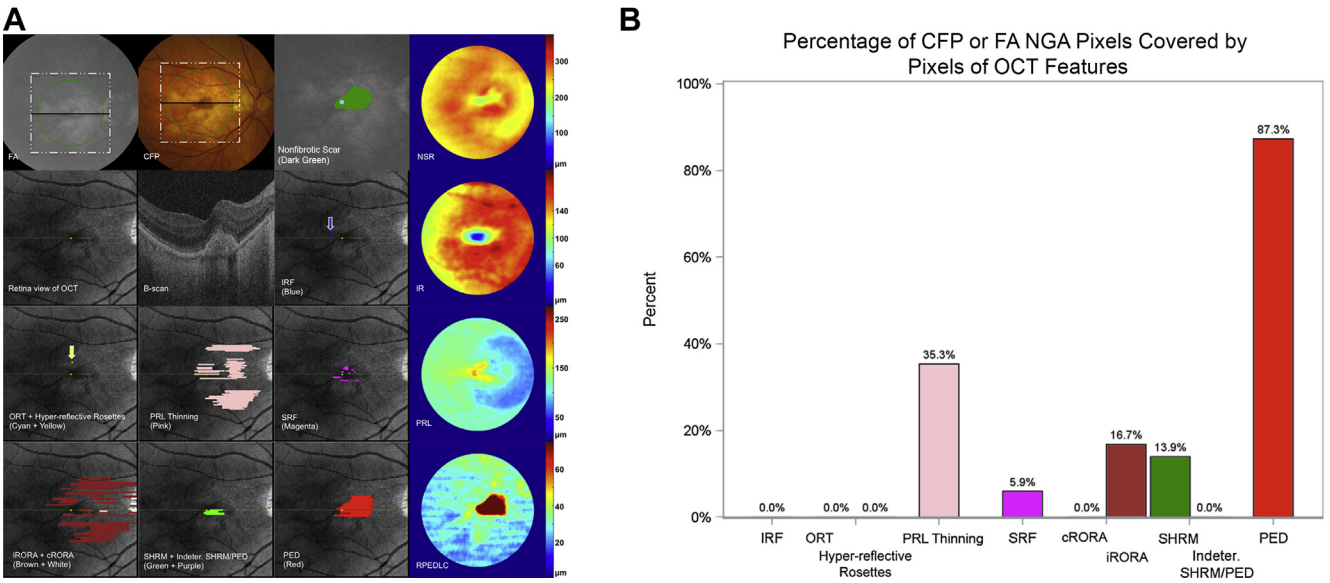

Figure 7. A, Images from a representative macula in an eye with a history of neovascular age-related macular degeneration obtained 2 years after the start of anti–vascular endothelial growth factor therapy. Nonfibrotic scar was identified on color fundus photography (CFP; row 1, column 2) and fluorescein angiography (FA; row 1, column 1, representative frame) review; the area of nonfibrotic scar was marked on a layer over the FA frame (row 1, column 3). The FA image was registered to the spectral-domain (SD) OCT retinal image (row 2, column 1). A representative B-scan (row 2, column 2) demonstrates 1 line of the SD-OCT morphologic features that were marked manually on each B-scan. Retinal changes on OCT included rare intraretinal fluid (IRF; row 2, column 3), outer retinal tubularization (ORT; row 3, column 1), and photoreceptor layer (PRL) thinning (row 3, column 2) corresponding to photoreceptor thinning on segmented scans (*dark blue*, row 3, column 4). Subretinal fluid (SRF; row 3, column 3) surrounded the subretinal highly reflective material (SHRM; row 4, column 2) over pigment epithelial detachment (PED; row 4, column 3). Incomplete retinal pigment epithelium (RPE) and outer retinal atrophy (iRORA; *brown*, row 4, column 1) was present despite more normal appearance of RPE on CFP or FA. The thickness of the SHRM and PED complex is reflected in the color map as an area of thickened RPE plus drusen plus lesion complex (RPEDLC; *dark red*, row 4, column 4). **B**, Graph showing the percentage of CFP- or FA-determined nonfibrotic scar lesion pixels covered by pixels of OCT features. cRORA = complete outer retinal atrophy; IR = inner retina; NSR = neurosensory retina.

of thickened RPEDLC (Fig 7A, dark red). Increased choroidal signal without loss of reflective material in the RPE location (Fig 7A, red-brown) involved some of the scar area and extended beyond.

In addition to the subretinal, RPE, and choroidal changes, SD-OCT also revealed patterns of retinal degeneration within the CFP- or FA-designated nonfibrotic scar area. Intraretinal fluid and hyperreflective rosettes (Fig 7A) were present focally. Photoreceptor layer thinning extended across some of the nonfibrotic scar area and beyond on qualitative maps (Fig 7A, pink), but less so centrally on the quantitative maps (Fig 7A, dark blue). Inner retinal layers were thickened over and beyond the area of photoreceptor thinning, and total retinal thickness was greatest in a ring surrounding the subretinal complex (Fig 7A, retinal thickness maps).

The percent of the nonfibrotic scar area covered by each SD-OCT feature is summarized in the graph in Figure 7B. More than 85% of the nonfibrotic scar area showed PED, 35% showed photoreceptor thinning, and a smaller area showed an increase in choroidal signal or SHRM. The RPEDLC thickness inside the 5-mm diameter ROI, meaning within the CFP or FA area designated as nonfibrotic scar, was 96.4 μm (standard deviation, 43.9 μm).

Discussion

Rather than analyzing AMD lesion component and OCT data from the macula as a whole or by rings or quadrants, using these new methods, we were able to colocalize SD-OCT–determined and CFP- or FA-determined pathologic features in precise pixel locations across the macula. We were able to apply these techniques in nAMD eyes treated with anti-VEGF therapy for 2 years. We also were able to determine thickness of retinal layers and thickness of the RPEDLC within the same pixel designations across the macula. These techniques enabled visualization and analysis that revealed novel information about the colocalization of OCT features and layer thicknesses within areas of CFP or FA designated as atrophy and scar. This information is of great interest for larger studies because of the association between poorer visual acuity in eyes with atrophy or scar after 2 years of anti-VEGF treatment. These methods will be useful not only for cross-sectional study, but also in longitudinal analyses to determine precursor morphologic features leading to atrophy or fibrosis at the site of or adjacent to a neovascular complex.

In everyday clinical practice or research analysis, it is difficult to appreciate, on a review of OCT B-scans or of a retinal volume, the relationship between multilayer morphologic changes relative to the location of an adjacent subretinal complex or the extent of combined pathologic changes (e.g., photoreceptor thinning along with increased choroidal signal). With segmentation and visualization of the areas and volumes of change, one can appreciate the broad extent and interrelationships of multiple pathologic features. The pixel-to-pixel correspondence of the regions of CFP or FA lesion components, OCT features, and

thickening and thinning of layers enables location-specific lesion analyses across groups of eyes or of the same eye over time. In the future, results of such analyses in longitudinal clinical trials will identify the critical feature combinations that predict outcomes. The clinician will not need to analyze all combinations of features, but will have analytic programs that will seek the significant combinations of features to guide treatment.

In these examples, the OCT-determined location of a persisting subretinal complex could be mapped within the area designated as GA on CFP or FA, and the thickness of RPEDLC and retinal layers could be extracted for the representative pixels. The data from these few eyes point to the recognized inaccuracy of the term *geographic atrophy* to describe an eye undergoing treatment for nAMD and in which the CFP or FA appearance is as defined in Table 1. Although the photographic and angiographic appearance may not be distinguishable from that of GA, the analysis of the RPE, choroidal signal, and thickness of the admixture of RPE and subretinal lesion together distinguish these examples from conventional GA. An alternate term such as *macular atrophy* is more appropriate in eyes with macular nAMD. Larger studies applying these methods will improve our understanding of the coincident features and thicknesses within macular atrophy.

Morphologic changes may extend over and well beyond regions of treated CNVL and often are not appreciated without such visualizations. A notable finding in this initial pilot analysis is the presence of extended areas of retinal thinning and of hyperreflective rosettes and tubulation not only in eyes with GA and non-GA, but also in eyes with scar. Another OCT morphologic change is the loss of RPE absorption of the light (even in the thicker subretinal lesions) resulting in greater deep choroidal reflectance on OCT and likely contributing to the photographic appearance of GA. Across a larger group of eyes, we will explore the relationships between these areas and overlying photoreceptor loss and other morphologic features and visual acuity outcomes. In addition to providing a method for visualization, these methods provide the ability to extract relative component areas, comparable thicknesses, and volumes that can be analyzed across groups of eyes to determine, for example, the mean and standard deviation of thickness of the RPEDLC within a lesion area or relative to retinal layer changes and angiographic or photographic changes. In future studies, it will be of interest to analyze findings in areas of lesion activity whether on CFP or FA or on OCT as fluid, whether intraretinal, subretinal, or sub-RPE. We will use this analysis to compare lateral and axial dimensions of thickened and thinned RPEDLC and change over time. Autofluorescent or other en face imaging methods also can be integrated into this analysis.

This information may be important in distinguishing pathways of local retinal damage and early retinal imaging markers for these pathways and their timeline relative to vision loss. A limitation of this study is the lack of functional testing such as with microperimetry across the regions of retinal and subretinal morphologic characteristics. Functional testing would be valuable in future studies of noncentral regions of disease. There are several additional limitations to this study. Multimodal imaging of the macula such as with blue or near-infrared autofluorescence[19,20] or of macular pigment were not captured in CATT. The processes of registration and correction of segmentation are all time intensive and challenging in eyes with nAMD. Improving automation of software and larger studies to determine which characteristics are useful as biomarkers will streamline future image processing and analysis.

There have been comparable studies examining select SD-OCT characteristics when compared with CFP or FA; however, none have considered the interaction between multiple factors by precise location.[1,2,4–8,21,22] Other methods to visualize OCT characteristics of complete RPE and outer retinal atrophy mapping with polarization-sensitive OCT require specialized equipment, and although it would allow visualization of RPE components and subretinal fibrosis, it would not enable analysis of these multiple intraretinal and subretinal components.[23,24] OCT angiography brings additional information to the analysis of sites of vascular flow such as within the neovascular complex, but does not further the analysis of nonvascular tissues.[25]

Extending this analysis to a series of eyes using this method of masked independent mapping of CFP, FA, and OCT lesion components will aid in defining the relationships between multiple OCT characteristics and between these and CFP or FA determination of lesions. Furthermore, following up such mapping over time will allow us to study the local precursors to the development of GA, fibrotic scar, and retinal thinning, all of which are associated with poorer functional outcomes. Greater understanding of the changes associated with loss of vision may lead to the identification of better treatment strategies.

References

1. Daniel E, Toth CA, Grunwald JE, et al. Risk of scar in the Comparison of Age-Related Macular Degeneration Treatments Trials. *Ophthalmology*. 2014;121:656–666.
2. Grunwald JE, Daniel E, Huang J, et al. Risk of geographic atrophy in the Comparison of Age-Related Macular Degeneration Treatments Trials. *Ophthalmology*. 2014;121:150–161.
3. Maguire MG, Martin DF, Ying GS, et al. Five-year outcomes with anti-vascular endothelial growth factor treatment of neovascular age-related macular degeneration: the Comparison of Age-Related Macular Degeneration Treatments Trials. *Ophthalmology*. 2016;123:1751–1761.
4. Jaffe GJ, Martin DF, Toth CA, et al. Macular morphology and visual acuity in the Comparison of Age-Related Macular Degeneration Treatments Trials. *Ophthalmology*. 2013;120:1860–1870.
5. Sharma S, Toth CA, Daniel E, et al. Macular morphology and visual acuity in the second year of the Comparison of Age-Related Macular Degeneration Treatments Trials. *Ophthalmology*. 2016;123:865–875.
6. Mowatt G, Hernandez R, Castillo M, et al. Optical coherence tomography for the diagnosis, monitoring and guiding of treatment for neovascular age-related macular degeneration: a systematic review and economic evaluation. *Health Technol Assess*. 2014;18:1–254.
7. Schmidt-Erfurth U, Waldstein SM. A paradigm shift in imaging biomarkers in neovascular age-related macular degeneration. *Prog Retin Eye Res*. 2016;50:1–24.

8. Castillo MM, Mowatt G, Elders A, et al. Optical coherence tomography for the monitoring of neovascular age-related macular degeneration: a systematic review. *Ophthalmology*. 2015;122:399–406.
9. CATT Research Group; Martin DF, Maguire MG, Fine SL, et al. Ranibizumab and bevacizumab for neovascular age-related macular degeneration. *N Engl J Med*. 2011;364:1897–1908.
10. CATT Research Group; Martin DF, Maguire MG, Fine SL, et al. Ranibizumab and bevacizumab for treatment of neovascular age-related macular degeneration: two-year results. *Ophthalmology*. 2012;119:1388–1398.
11. Folgar FA, Jaffe GJ, Ying GS, et al. Comparison of optical coherence tomography assessments in the comparison of age-related macular degeneration treatments trials. *Ophthalmology*. 2014;121:1956–1965.
12. Grunwald JE, Daniel E, Ying GS, et al. Photographic assessment of baseline fundus morphologic features in the Comparison of Age-Related Macular Degeneration Treatments Trials. *Ophthalmology*. 2012;119:1634–1641.
13. Holz FG, Sadda SR, Staurenghi G, et al. Imaging protocols in clinical studies in advanced age-related macular degeneration: recommendations from Classification of Atrophy Consensus Meetings. *Ophthalmology*. 2017;124:464–478.
14. DeCroos FC, Toth CA, Stinnett SS, et al. Optical coherence tomography grading reproducibility during the Comparison of Age-Related Macular Degeneration Treatments Trials. *Ophthalmology*. 2012;119:2549–2557.
15. Farsiu S, Chiu SJ, O'Connell RV, et al. Quantitative classification of eyes with and without intermediate age-related macular degeneration using optical coherence tomography. *Ophthalmology*. 2014;121:162–172.
16. Jain N, Farsiu S, Khanifar AA, et al. Quantitative comparison of drusen segmented on SD-OCT versus drusen delineated on color fundus photographs. *Invest Ophthalmol Vis Sci*. 2010;51:4875–4883.
17. Chiu SJ, Izatt JA, O'Connell RV, et al. Validated automatic segmentation of AMD pathology including drusen and geographic atrophy in SD-OCT images. *Invest Ophthalmol Vis Sci*. 2012;53:53–61.
18. Willoughby AS, Ying GS, Toth CA, et al. Subretinal hyperreflective material in the Comparison of Age-Related Macular Degeneration Treatments Trials. *Ophthalmology*. 2015;122:1846–1853.e5.
19. Pilotto E, Guidolin F, Convento E, et al. En face optical coherence tomography to detect and measure geographic atrophy. *Invest Ophthalmol Vis Sci*. 2015;56:8120–8124.
20. Ben Moussa N, Georges A, Capuano V, et al. MultiColor imaging in the evaluation of geographic atrophy due to age-related macular degeneration. *Br J Ophthalmol*. 2015;99:842–847.
21. Keane PA, Liakopoulos S, Chang KT, et al. Comparison of the optical coherence tomographic features of choroidal neovascular membranes in pathological myopia versus age-related macular degeneration, using quantitative subanalysis. *Br J Ophthalmol*. 2008;92:1081–1085.
22. Sadda SR, Liakopoulos S, Keane PA, et al. Relationship between angiographic and optical coherence tomographic (OCT) parameters for quantifying choroidal neovascular lesions. *Graefes Arch Clin Exp Ophthalmol*. 2010;248:175–184.
23. Schutze C, Teleky K, Baumann B, et al. Polarisation-sensitive OCT is useful for evaluating retinal pigment epithelial lesions in patients with neovascular AMD. *Br J Ophthalmol*. 2016;100:371–377.
24. Roberts P, Sugita M, Deak G, et al. Automated identification and quantification of subretinal fibrosis in neovascular age-related macular degeneration using polarization-sensitive OCT. *Invest Ophthalmol Vis Sci*. 2016;57:1699–1705.
25. Coscas GJ, Lupidi M, Coscas F, et al. Optical coherence tomography angiography versus traditional multimodal imaging in assessing the activity of exudative age-related macular degeneration: a new diagnostic challenge. *Retina*. 2015;35:2219–2228.

Footnotes and Financial Disclosures

Originally received: February 24, 2017.
Final revision: September 19, 2017.
Accepted: September 21, 2017.
Available online: November 28, 2017. Manuscript no. ORET_2017_54.

[1] Department of Ophthalmology, Duke University, Durham, North Carolina.

[2] Department of Ophthalmology, University of Pennsylvania, Philadelphia, Pennsylvania.

[3] Cole Eye Institute, Cleveland Clinic, Cleveland, Ohio.

[4] Department of Biomedical Engineering, Duke University, Durham, North Carolina.

*A complete listing of the clinical centers and the members of the Comparison of Age-Related Macular Degeneration Treatments Trials group is available at www.ophthalmologyretina.org.

Financial Disclosure(s):
The author(s) have made the following disclosure(s): C.A.T.: Financial support — Genentech; royalties — Alcon/Novartis

S.J.C.: Patent — Segmentation and identification layered structures in images

G.J.J.: Financial support — Heidelberg Engineering

G-s.Y.: Financial support — Janssen Research & Development, Chengdu Kanghong Biotech Co.

Supported by the National Eye Institute, National Institutes of Health, Bethesda, Maryland (cooperative agreement nos.: U10 EY017823, U10 EY017825, U10 EY017826, and U10 EY01782). Its contents are solely the responsibility of the authors and do not necessarily represent the official view of National Eye Institute, National Institutes of Health, or the Department of Health and Human Services. The sponsors or funding organizations had no role in the design or conduct of this research.

Human Subjects: Human subjects were included in this study. No animal subjects were used in this study. The study was approved by an institutional review board associated with each center and complied with the Health Insurance Portability and Accountability Act regulations. The study was performed in accordance with the tenents of the Declaration of Helsinki. All participants provided written informed consent.

Author Contributions:

Conception and design: Toth, Sevilla, Daniel, Jaffe, Martin, Pistilli, Farsiu, Maguire

Analysis and interpretation: Toth, Tai, Winter, Daniel, Grunwald, Ying, Pistilli, Maguire

Data collection: Toth, Tai, Chiu, Winter, Sevilla, Daniel, Ying, Pistilli, Maguire

Obtained funding: N/A

Overall responsibility: Toth, Tai, Chiu, Winter, Sevilla, Daniel, Grunwald, Jaffe, Martin, Ying, Pistilli, Farsiu, Maguire

Abbreviations and Acronyms:
AMD = age-related macular degeneration; **CATT** = Comparison of Age-Related Macular Degeneration Treatments Trials; **CFP** = color fundus photography; **FA** = fluorescein angiography; **GA** = geographic atrophy; **iRORA** = incomplete retinal pigment epithelium and outer retinal atrophy; **nAMD** = neovascular age-related macular degeneration; **OPL** = outer plexiform layer; **ROI** = region of interest; **RPE** = retinal pigment epithelium; **RPEDLC** = retinal pigment epithelium plus drusen plus lesion complex; **SD-OCT** = spectral-domain OCT; **SHRM** = subretinal highly reflective material; **VEGF** = vascular endothelial growth factor.

Correspondence:
Cynthia A. Toth, MD, Department of Ophthalmology, Duke University Medical Center, 2351 Erwin Road, Box 3802, Durham, NC 27710. E-mail: cynthia.toth@dm.duke.edu.

Pictures & Perspectives

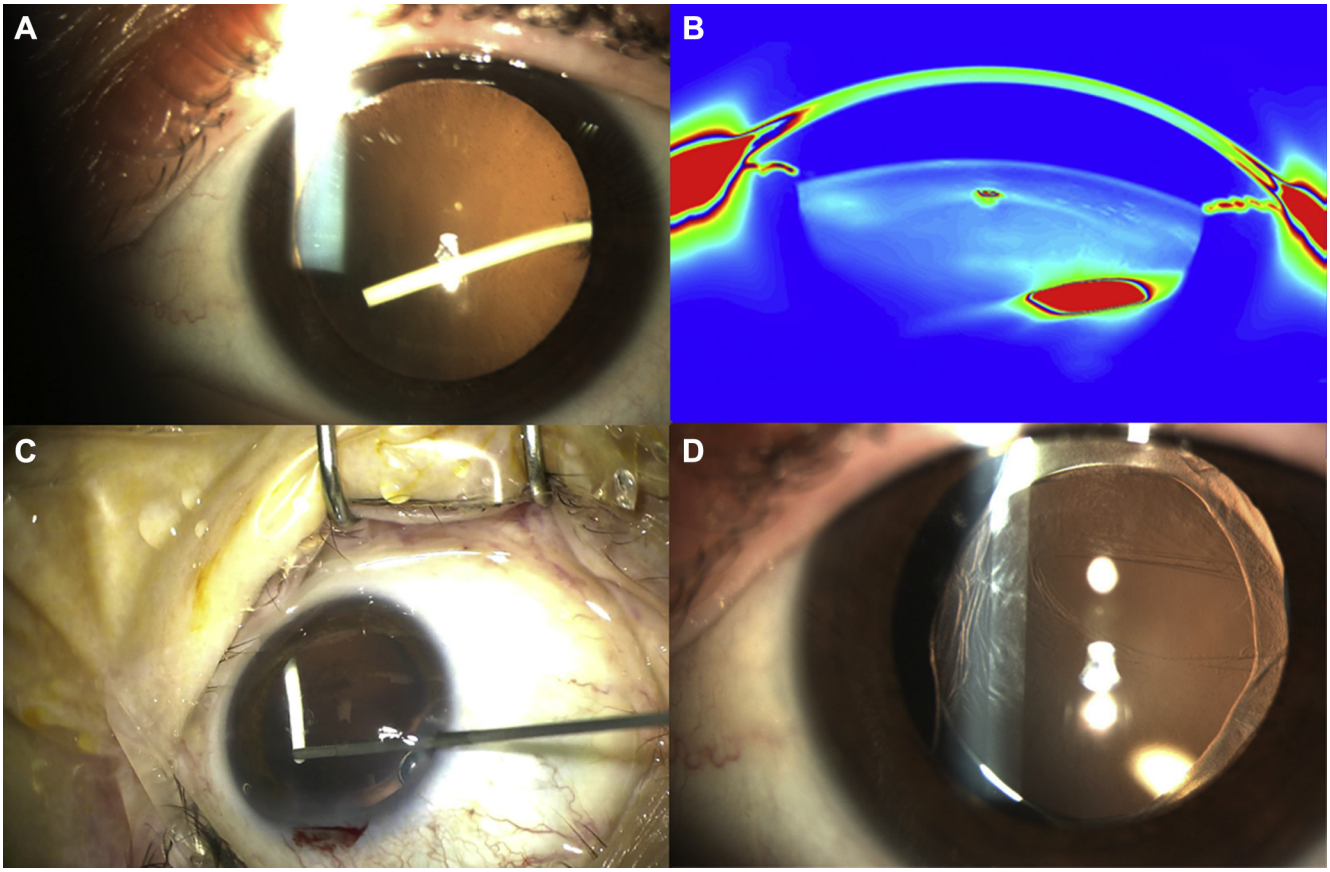

A Case of Inadvertent Intralenticular Dexamethasone Implant

A 59-year-old woman was referred with left branch retinal vein occlusion with macular edema. She underwent an intravitreal injection of dexamethasone implant. During this process the implant was inadvertently injected into the crystalline lens (Fig 1**A**). Scheimpflug imaging confirmed the intralenticular location of the dexamethasone implant (Fig 1**B**). She underwent an uncomplicated lens extraction with intraocular lens implantation and repositioning of the dexamethasone implant into the vitreous cavity (Fig 1**C**). At 1 month follow up, there was resolution of macular edema and at 6 months follow up the intraocular lens was stable in the capsular bag (Fig 1**D**).

Lin Wei Khoo, MBChB
Sathish Srinivasan, FRCSEd, FRCOphth
Zachariah Koshy, DNB, FRCSG
University Hospital Ayr, Ayr, Scotland, United Kingdom